Advanced Synthesis & Catalysis

Title: Silylation of Aryl Chlorides by Bimetallic Catalysis of Palladium and Gold on Alloy Nanoparticles

Authors: Hiroki Miura, Yosuke Masaki, Yohei Fukuta, and Tetsuya Shishido

To be cited as: *Adv. Synth. Catal.* 10.1002/adsc.202000045

Link to VoR: http://dx.doi.org/10.1002/adsc.202000045

Advanced Synthesis & Catalysis
10.1002/adsc.202000045

DOI: 10.1002/adsc.201((will be filled in by the editorial staff))

Silylation of Aryl Chlorides by Bimetallic Catalysis of Palladium and Gold on Alloy Nanoparticles

Hiroki Miura,[a,b,d,]* Yosuke Masaki,[a] Yohei Fukuta[a] and Tetsuya Shishido[a,b,c,d,]*

[a] Department of Applied Chemistry for Environment, Graduate School of Urban Environmental Sciences, Tokyo Metropolitan University, 1-1 Minami-Osawa, Hachioji, Tokyo 192-0397, Japan
E-mail: miura-hiroki@tmu.ac.jp, shishido-tetsuya@tmu.ac.jp
[b] Research Center for Hydrogen Energy-based Society, Tokyo Metropolitan University, 1-1 Minami-Osawa, Hachioji, Tokyo 192-0397, Japan
[c] Research Center for Gold Chemistry, Tokyo Metropolitan University, 1-1 Minami-Osawa, Hachioji, Tokyo 192-0397, Japan
[d] Elements Strategy Initiative for Catalysts & Batteries, Kyoto University, Katsura, Nishikyo-ku, Kyoto 615-8520, Japan

Received: ((will be filled in by the editorial staff))

Supporting information for this article is available on the WWW under http://dx.doi.org/10.1002/adsc.201######.

Abstract. Supported palladium–gold alloy-catalyzed cross-coupling of aryl chlorides and hydrosilanes enabled the selective formation of aryl–silicon bonds. Whereas a monometallic palladium catalyst predominantly promoted the hydrodechlorination of aryl chlorides and gold nanoparticles showed no catalytic activity, gold-rich palladium–gold alloy nanoparticles efficiently catalyzed the title reaction to give arylsilanes with high selectivity. A wide array of aryl chlorides and hydrosilanes participated in the heterogeneously-catalyzed reaction to furnish the corresponding arylsilanes in 34-80% yields. A detailed mechanistic investigation revealed that palladium and gold atoms on the surface of alloy nanoparticles independently functioned as active sites for the formation of aryl nucleophiles and silyl electrophiles, respectively, which indicates that palladium and gold atoms on alloy nanoparticles work together to enable the selective formation of aryl–silicon bonds.

Keywords: silylation; cross-coupling; aryl chloride; alloy nanoparticles; heterogeneous catalyst

Introduction

Arylsilanes are an important class of molecules due to their property for components of organic light emitting diodes.[1–3] Furthermore, established synthetic methods, such as Hiyama cross-coupling reactions, enable facile transformation of these compounds to high value-added compounds, such as natural products, drugs, and functional materials.[4] Despite the high efficiency of the nucleophilic attack of Grignard and organolithium reagents to Si electrophiles (Scheme 1a, route 1), severe obstacles regarding stoichiometric amount of metallic reagents, the limitations of functional groups and the prefunctionalization of substrates reduce their reliability for introducing a silyl moiety into aromatics. Consequently, cross-coupling reactions of aryl and silyl moieties under the influence of transition-metal catalysts have appeared to be a sustainable tool for the formation of aryl–Si bonds.[5–9] While the direct silylation of an aromatic C–H bond with hydrosilanes is the most straightforward and atom-economical route to arylsilanes (Scheme 1a, route 2),[10–13] the inability to control the regiochemistry and the narrow substrate scope decrease their versatility. In contrast, the substitution of an aryl-halide bond to an aryl–Si bond, namely the cross-coupling of aryl halides with hydrosilanes, is the most reliable method for the regio-controlled silylation of arenes. Particularly,

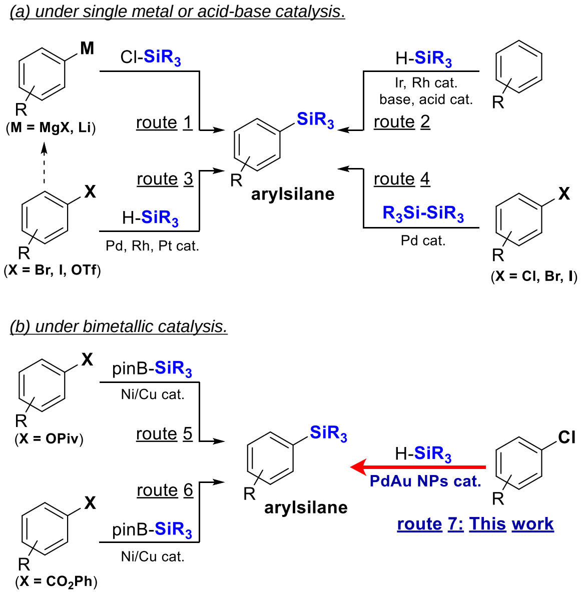

Scheme 1. Synthetic routes for arylsilanes

appropriate combinations of transition metals, such as Pd,[14–21] Rh[22–28] and Pt,[29,30] and bulky phosphine ligands enable the catalytic silylation of aryl halides bearing various functional groups while avoiding undesired hydrodehalogenation (Scheme 1a, route 3). However, nearly all investigations of the title reaction have been limited to the use of reactive bromides, iodides and triflates as an aryl source. Although aryl chlorides are undoubtedly expedient substrates in view of their low cost and wide availability, their application is still difficult due to the higher dissociation energy of the C–Cl bond compared to those of C–Br and C–I.[31,32] Although the cross-coupling reaction of aryl chlorides and disilanes has been reported as an alternative method for the silylation of aryl chlorides (Scheme 1a, route 4),[33,34] the limited variety of disilanes still requires an efficient silylation via the cross-coupling of aryl chlorides and hydrosilanes. However, the fact that metal complex catalysts with activities that can be tuned by the choice of suitable ligand have not provided definite solutions to date implies that some as-yet unexplored approach may be needed to devise a novel protocol for C–Si bond formation. On the other hand, bimetallic catalysis has recently attracted considerable attention as a powerful tool for realizing unprecedented molecular transformations.[35–39] The groups of Martin and Rueping independently reported efficient aryl–Si bond formation via the coupling of aryl esters and silyl boranes under Ni/Cu bimetallic catalysis,[40,41] which includes C–O bond and Si–B bond activation by Ni and Cu, respectively (Scheme 1b, routes 5 and 6). On the other hand, much attention has been focused on the reaction under the influence of heterogeneous catalysts from the perspective of green and sustainable chemistry thanks to high reusability of the catalysts and low contamination of toxic metals into valuable chemicals. We recently demonstrated the unique catalytic functions of bimetallic nanoparticles (NPs) for efficient organic transformations.[42–45] In the course of our study on the PdAu alloy-catalyzed hydrosilylation of unsaturated organic molecules, we found that highly electrophilic silyl species could form on Au atoms on the surface of NPs, which realized an efficient silylation of organic molecules.[42,43] Furthermore, Sakurai and co-workers reported the low-temperature activation of an aryl–Cl bond under the catalysis of well-defined PdAu bimetallic nanoclusters.[46–49] These findings enabled us to envision an efficient formation of aryl–Si bonds from aryl chlorides under the bimetallic catalysis of adjacent Pd and Au atoms on the surface of PdAu alloy NPs(Scheme 1b, route 7). Herein, we describe an efficient method for synthesizing arylsilanes via the cross-coupling of aryl chlorides and hydrosilanes in the presence of supported PdAu alloy NPs catalysts. A variety of arylsilanes could be synthesized by using PdAu bimetallic catalysis without the aid of phosphine ligands. The surface composition of Pd and Au atoms on the alloy NPs affected the selectivity for arylsilanes, and alloy NPs with high Au concentration were crucial for the selective formation of aryl–Si bonds while avoiding the reduction of aryl–Cl bonds.

Results and Discussion

Supported PdAu alloy catalysts (xPdyAu/support: x and y denote the molar ratio of Pd to Au.) were prepared through a sol-immobilization method. The PdAu NPs with mean diameters of about 3 nm were highly dispersed on the surface of each support, and no significant differences in the mean diameter of alloy NPs were confirmed when the Pd/Au ratio of alloy NPs was varied.[42,50] Table 1 summarizes the effect of metallic components of NPs and their support on the cross-coupling of chlorobenzene (**1a**) with triethylsilane (**2a**) in the presence of Na_2CO_3 (2.0 eqiuv) as a base. Monometallic Pd NP catalyst predominantly underwent hydrodechlorination to form benzene (**4a**), resulting in a quite low yield of the target product (**3aa**) (entry 1). On the other hand, alloying Pd with Au improved the selectivity for **3aa**, and the values increased with an increase in the Au concentration in PdAu alloy NPs (entries 2–5). Although the conversion rate was decreased, the highest selectivity was obtained in the reaction with the 1Pd6Au catalyst. Monometallic Au NPs showed no activity for the cross-coupling reaction (entry 6). Our previous works on the detailed characterization of

Table 1. Silylation of chlorobenzene over supported catalysts.

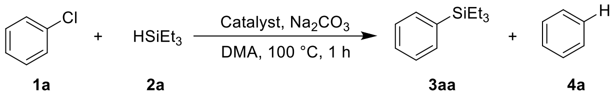

entry	catalyst	yield [%][b]		selectivity of
		3aa	**4a**	**3aa**/**3aa**+**4a** [%][b]
1	Pd/C	11	82	12
2	3Pd1Au/C	14	80	14
3	1Pd1Au/C	40	56	42
4	1Pd3Au/C	64	30	68
5	1Pd6Au/C	19 (66)[c]	4 (19)[c]	84 (77)[c]
6	Au/C	0	0	0
7	1Pd6Pt/C	0	2	0
8	1Ni6Au/C	0	2	0
9	1Cu6Au/C	0	2	0
10	$Pd_2(dba)_3$	30	46	40
11	$Pd_2(dba)_3$ + Au/C	57	28	67
12	$1Pd6Au/Nb_2O_5$	9	3	74
13	$1Pd6Au/Al_2O_3$	29	8	78
14	$1Pd6Au/TiO_2$	33	11	75
15	$1Pd6Au/ZrO_2$	34 (77)[d]	13 (18)[d]	73 (81)[d]

[a] Reaction conditions: **1a** (0.5 mmol), **2a** (2.5 mmol), catalyst (2.0 mol% as metal), Na_2CO_3 (1.0 mmol), DMA (1 mL), at 100 ℃. [b] Yields and selectivities of the products were determined by GC analysis by using *n*-decane as internal standard. [c] Reaction for 6 h. [d] Reaction for 3 h.

PdAu alloy NPs revealed that Pd and Au were uniformly mixed in the nanoparticle to random alloy structure.[42–45, 50] PdPt NPs have also been reported to form random alloy, while PdPt NPs were totally ineffective toward the reaction (entry 7). Furthermore, supported NiAu and CuAu catalysts showed quite low activity. These results clearly indicate that the significance of the coexistence of Pd and Au for realizing the selective formation of an aryl–Si bond. Interestingly, although the reaction under the catalysis of soluble Pd(0) complex resulted in a low selectivity for **3aa** (entry 8), the addition of Au/C to the homogeneous Pd-catalyzed reaction improved the arylsilane selectivity (entry 9). If we consider the quite low activity for activating the C-Cl bond and significant activity for cleaving the Si-H bond of Au NPs,[51–55] Pd and Au are anticipated to activate aryl chloride and hydrosilane, respectively. After careful screening of the supporting materials for 1Pd6Au NPs (entry 10–13), ZrO_2 was found to be the optimal support to give **3aa** in 77% yield after the reaction for 3 h at 100 °C. Evaluation of the adsorption rate of chlorobenzene (**1a**) onto supports helped to elucidate the effect of the supports (Figure S1). The adsorption rate of **1a** onto supports positively correlated with the formation rate of both **3aa** and **4a**. Moreover, we revealed that the formation-rate limiting step for arylsilanes in the title reaction was oxidative addition of aryl chlorides (vide infra). These facts enabled us to deduce that acidic or basic property of ZrO_2 increased the concentration of aryl chlorides at around catalytically active PdAu NPs, thereby leading high catalytic performance of PdAu/ZrO_2. Notably, DMA, DMF, NMP and CH_3CN, were suitable solvents for the present reaction, while toluene, 1,4-dioxane and DMSO were totally ineffective.[56]

The unique catalysis by PdAu NPs for synthesizing arylsilanes is reflected only in the reaction of aryl chlorides as starting substrates (Table 2). The reaction of bromobenzene (**1a’**) with **2a** resulted in a moderate selectivity for **3aa**. Besides, the reaction of iodobenzene (**1a’’**) did not afford **3aa** since reduction or homo-coupling proceeded predominantly to give benzene and biphenyl, respectively. These results suggest that specific interaction between PdAu NPs and chloride anion should be involved in the catalytic cycles for the selective formation of aryl–Si bonds (vide infra).With the optimized catalyst in hand, the scope of substrates in the cross-coupling of aryl chlorides with hydrosilanes was examined (Table 3). A series of triethylsilyl arenes could be synthesized. Furthermore, the present PdAu catalytic system could be employed on a gram scale to furnish **3ba** in a yield of 55% (1.13 g of **3ba** was isolated). The electronic nature of the substituents on arenes slightly influenced both the conversion rate of aryl chlorides and the yields of the silylated products. As generally observed in the present catalytic reactions, aryl chlorides bearing electron-donating substituents, such as methyl and methoxy groups, gave the corresponding products (**3ba**–**3ea**) in high yields, although the reactions required a long time to run to completion. A fluoro substituent positively affected the yield of the product

Table 2. Silylation of aryl halides over supported PdAu catalysts.[a)]

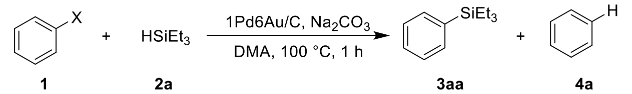

entry	1	yield [%][b]		selectivity of 3aa/3aa+4a [%][b]
		3aa	4a	
1	**1a** (X=Cl)	19	4	84
2	**1a'** (X=Br)	37	32	54
3	**1a''** (X=I)	1	39	2[c]

[a] Reaction conditions: **1** (0.5 mmol), **2a** (2.5 mmol), 1Pd6Au/C (2.0 mol% as metal), Na_2CO_3 (1.0 mmol), DMA (1 mL), at 100 ℃. [b]Yields and selectivities of the products were determined by GC analysis by using *n*-decane as internal standard. [c] Biphenyl was formed as a by-product in 31% yield.

Table 3. Scope of substrates[a)]

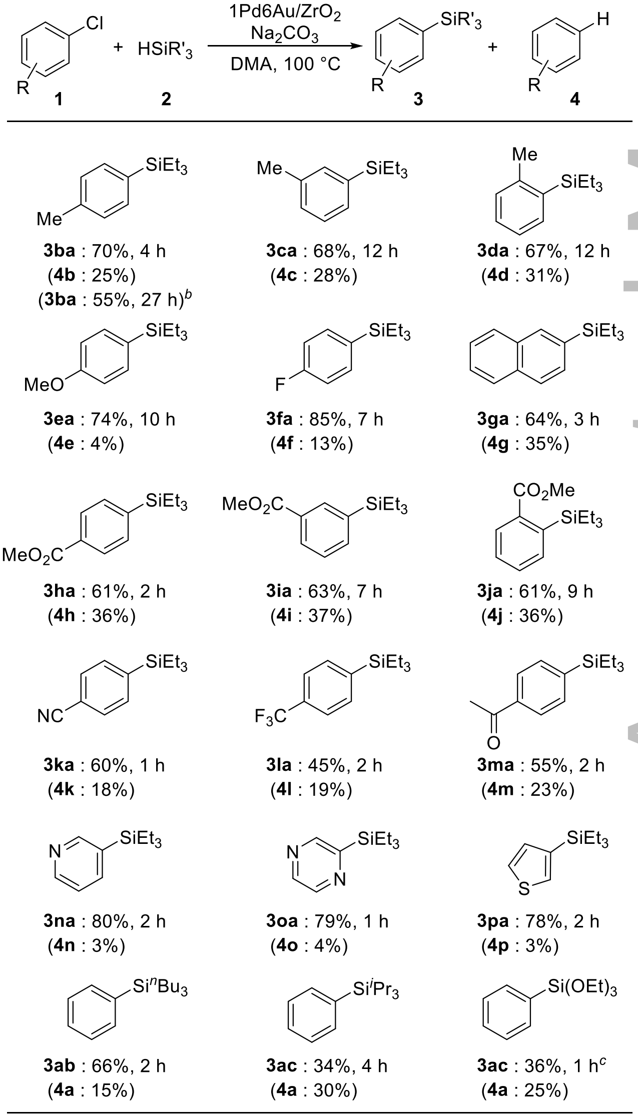

[a]Reaction conditions: **1** (0.50 mmol), **2** (2.5 mmol), 1Pd6Au/ZrO_2 (2.0 mol% as metal), Na_2CO_3 (1.0 mmol), DMA (1 mL), at 100 ºC. Isolated yields were given. [b]Reaction run at 20 times the scale as that used in the standard reaction conditions. [c]Hydrosilane was added dropwise.

3fa. Silyl naphthalene (**3ga**) was also obtained in 64% yield. In contrast, the reactions of aryl chlorides with electron-withdrawing substituents afforded the corresponding arylsilanes (**3ha**–**3ma**) in slightly reduced yields, and the reactions went to completion quickly. Importantly, reactive functionalities, such as ester, nitrile and ketone, remained intact during the PdAu-catalyzed silylation. The position of a methyl or ester substituent on arenes did not affect the yield of the final product (**3ba**–**3da** and **3ha**–**3ja**), suggesting that steric hindrance around the C–Cl bond is not a crucial factor for determining the chemoselectivity. The significance of the present protocol was well-reflected in the formation of heteroaryl–Si bonds. Silyl pyridine, pyrazine and thiophene were obtained in around 80% yields. Facile adsorption of heteroaryl substrates onto PdAu NPs due to the positive interaction of N and S atoms with PdAu NPs would promote the rate-limiting step in the present catalytic reaction. Several silyl coupling partners other than triethylsilane could also be accommodated to give the corresponding arylsilanes, while aryl-substituted hydrosilanes, such as dimethylphenylsilane, diphenylsilane and phenylsilane, and silanes with bulky substituents, such as dimethyl tert-butylsilane were not good substrates in the PdAu NPs-catalyzed reaction. Notably, excess hydrosilanes were required to obtain arylsilanes in satisfactory yields, since water that is adsorbed on the support promotes the rapid hydrolytic conversion of hydrosilanes to silanols or siloxanes as the main side reaction to reduce the product yields. High temperatures that can remove the adsorbed water on the surface of solid catalysts cause the aggregation and segregation of PdAu NPs. Thus, we used the catalysts dried in oven below 100 ºC.

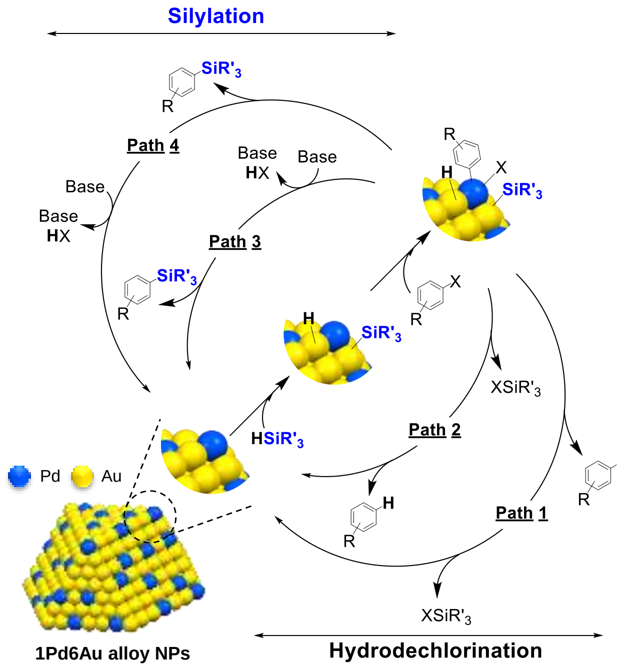

Scheme 2. The model structure of 1Pd6Au alloy nanoparticles and possible reaction pathway for the coupling reaction of aryl chlorides with hydrosilanes over PdAu catalysts.

To gain insight into the reaction mechanism and the bimetallic effects on product selectivity, we postulated the reaction pathways for both the silylation and hydrodehalogenation of aryl halides, as shown inScheme 2. Our previous detailed study on the structural characterization of PdAu NPs revealed that Pd and Au atoms were homogeneously mixed to form random alloy NPs.[42–45,50] Furthermore, hot-filtration of supported PdAu catalysts completely suppressed further progress of the reaction (see Fig. S4 in Supplementary Information), clearly indicating that the reaction took place on the surface of PdAu alloy NPs. The routes to arylsilanes and reduced arenes must include the dissociative adsorption of hydrosilanes and aryl halides on the surface of PdAu NPs, and H–Si bond activation should take place prior to cleavage of a C–X bond in view of the high dissociation energy of the C–X bond. The subsequent bond-forming steps (Paths 1–4 in Scheme 2) could be classified into two categories, for hydrodechlorination and silylation, each of which should be divided into two bond-forming paths, Path 1 (aryl–H → Si–X), Path 2 (Si–X → aryl–H), Path 3 (H–X → aryl–Si) and Path 4 (aryl–Si → H–X), and the rate for the first bond-forming step should dominate the selectivity for the products. We performed the following studies to uncover the factors for dominating the product selectivity.

Figure 1A shows the effect of the type of carbonate base on the formation rate and selectivity of arylsilane **3aa** in the cross-coupling of chlorobenzene (**1a**) and **2a**. Basicity affected the formation rate of **3aa**, and alkaline-metal carbonates with weak basicity, such as lithium and sodium salt, exhibited high formation rates for **3aa**. In contrast, there were no significant differences in the selectivity for **3aa**. Furthermore, as shown in Figure 1B, the amount of base also did not affect either the formation rate or the selectivity for **3aa**. These results suggest that the base does not participate

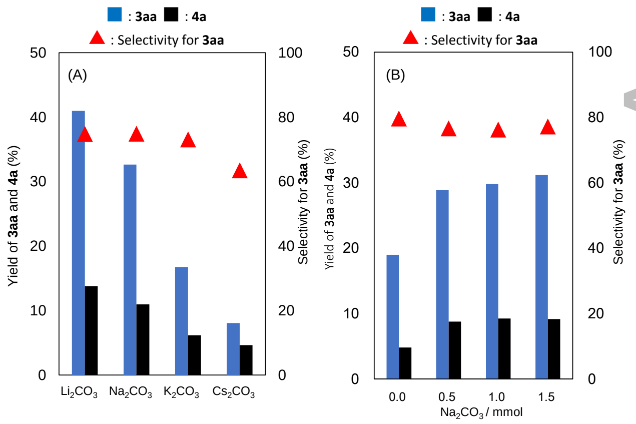

Figure 1. Effect of (A) a sort of carbonate base and (B) the amount of Na_2CO_3 on the formation-rate and the selectivity for the products (**3aa** and **4a**) in the coupling reaction of **1a** and **2a**. Reaction condition (A); **1a** (0.50 mmol), **2a** (2.5 mmol), 1Pd6Au/C (2.0 mol% as metal), base (1.0 mmol), DMA (1 mL), at 100 ^{o}C, for 1 h. (B) **1a** (0.50 mmol), **2a** (2.5 mmol), 1Pd6Au/C (2.0 mol% as metal), DMA (1 mL), at 100 ^{o}C, for 1 h. GC yields were given.

in the selectivity-determining step of the reaction of aryl chlorides and hydrosilanes. On the other hand, the substituent on the aromatic ring influenced the selectivity of the products (Figure 2). The formation rates of both arylsilane and reduced arene in the reaction of aryl chloride with an electron-withdrawing ester group (**1h**) were increased in comparison to that with an electron-donating methyl group (**1b**). In contrast, increased selectivity for arylsilane was achieved in the reaction of **1b**. This is consistent with the results shown in Table 3 and indicates that the electronic state of the aryl species formed on Pd atom of PdAu NPs through the cleavage of aryl–Cl bonds should be the dominant factor for determining the product selectivity in the coupling reaction of aryl chlorides and hydrosilanes. Based on these results, the silylation and hydrodechlorination of aryl chlorides are expected to proceed preferably through Paths 4 and 1, respectively. Hence, electron-rich aryl species formed on Pd atoms of PdAu NPs are considered to rapidly react with electrophilic silyl species formed on adjacent Au atoms, which leads to highly selective aryl–Si bond formation.

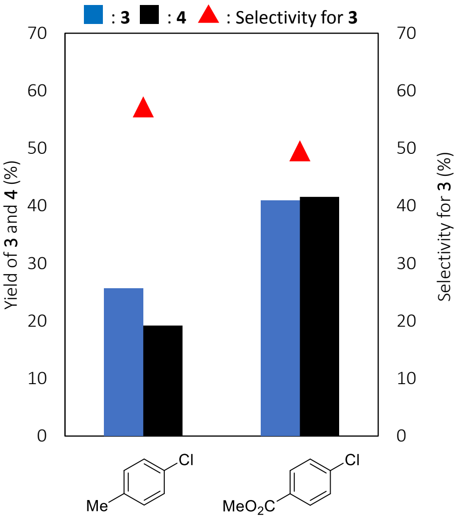

Figure 2. Effect of substituents on aryl chloride on the formation rate and selectivity for the products (3 and 4) in the coupling reaction of 1 and 2. Reaction conditions; 1 (0.50 mmol), 2 (2.5 mmol), 1Pd6Au/ZrO_2 (2.0 mol% as metal), Na_2CO_3 (1.0 mmol), DMA (1 mL), at r.t., for 1 h. GC yields are given.

Another key factor for product selectivity is the PdAu atomic ratio of PdAu alloy NPs, as shown in Table 1. As we previously reported regarding the hydrosilylation of unsaturated organic molecules over supported PdAu NPs,[42,43] the electronic state of Au in NPs can be varied by changing the Pd/Au atomic ratio.[50] Furthermore, electron-deficient Au atoms can be present in alloy PdAu NPs with a high Au concentration, and thus can form highly electrophilic silyl species on Au atoms in alloy PdAu NPs. As in the previous hydrosilylation over PdAu catalysts,[42,43] the formation of highly electrophilic silyl species on Au atoms facilitated aryl-Si bond formation to realize the highly selective silylation of aryl chlorides. Notably, the reaction-orders of **1a**, **2a** and Na_2CO_3 estimated from the formation rate of **3aa** were 0.6, -0.4 and -0.1, respectively. This indicates that the *formation rate*-determining step for arylsilanes in the reaction of aryl chlorides is undoubtedly oxidative addition of aryl chlorides, whereas the selectivity for arylsilanes should be determined in the step for desorbing each fragment.

We next focused on understanding the specific effect of halides in the reaction over PdAu alloy NPs. As shown in Table 2, highly selective silylation of aryl chlorides was seen only in the reaction of aryl chlorides, whereas the reactions of aryl bromides and iodides resulted in quite low arylsilane selectivity. The reaction-orders of bromobenzene (**1a'**), **2a** and Na_2CO_3 estimated from the formation rate of **3aa** were completely different from those for the reaction of aryl chlorides, with values of -0.4, 0.0 and 0.4, respectively. This indicates that both the formation-limiting and selectivity-determining steps in the reaction of aryl bromides should be different from those of aryl chlorides, and particularly, the rate-limiting step of the reaction would not be cleavage of the aryl–Br bond, but rather the bond-forming step. As shown in Figure 3A, the amount of base affected the selectivity for the product, and an increase in the amount of base increased the selectivity for arylsilane. In contrast, the substituents on the aromatic ring did not impact either the formation rate or the selectivity for arylsilane. These results suggest that the product selectivity in the reaction of aryl bromides is dominated, not by the electronic state of aryl species, but rather by the base, and that arylsilanes and reduced arenes are likely to be formed preferentially through Paths 3 and 2 in Scheme 2, respectively.

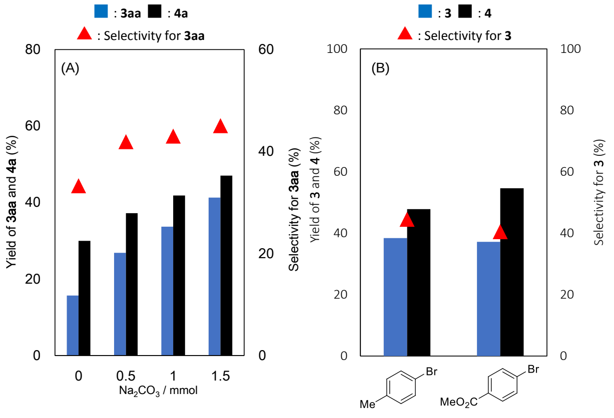

Figure 3. Effects of (A) the amount of Na_2CO_3 and (B) the substituents on aryl bromide on the formation rate and selectivity for the products (**3** and **4**) in the coupling reaction of bromobenzene and **2a**. Reaction conditions; **1** (0.50 mmol), **2a** (2.5 mmol), 1Pd6Au/ZrO_2 (2.0 mol% as metal), base (1.0 mmol), DMA (1 mL), at 100 ºC, for 40 min. GC

Although the exact reason for the specific effect of halogen in the reaction over PdAu alloy NPs is still not fully understood, we surmise that the difference in the ion radius between bromide and chloride ions remarkably affects their reactivities. The selectivity-determining step in the reaction of aryl bromides includes the desorption of Br from PdAu alloy NPs (Paths 2 and 3 in Scheme 2). In contrast, desorption of Cl is not involved in either Path 1 or Path 4 of the selectivity-determining step of silylation of aryl chlorides. This is probably because large bromide and silyl ions preferentially desorb from the surface to avoid steric repulsion between bulky PdAu NPs. In fact, the reaction of 1-chloro-4-iodobenzene and triethylsilane (**2a**) by 1Pd6Au/ZrO_2 catalyst predominantly gave chlorobenzene, which suggests that hydrodeiodation proceeded much faster than the silylation of C-Cl bond. In contrast, detailed theoretical studies on the homocoupling of aryl chloride over PdAu clusters by Ehara and Sakurai et al. proposed that the chloride ion was adsorbed at the interface of Pd and Au atoms. This suggests that such specific interaction between chloride ion and PdAu NPs helps to stabilize chloride anion at the surface of PdAu, thus resulting in highly selective silylation of aryl chlorides. Detailed theoretical investigations on the interaction of halogen and PdAu alloy NPs in the present reactions are currently underway in our laboratory.

Conclusion

We have described a highly selective silylation of aryl chlorides over supported PdAu NPs catalysts. Whereas monometallic Pd NPs predominantly promoted the hydrodechlorination of aryl chlorides to give reduced arenes and monometallic Au NPs showed no catalytic activity, PdAu alloy catalysts with high Au concentrations promoted the highly selective silylation of aryl–Cl bonds via the cross-coupling of aryl chlorides and hydrosilanes without the aid of phosphine ligands. A detailed mechanistic investigation unveiled that nucleophilic aryl species and electrophilic silyl species formed on Pd and Au atoms on the surface of PdAu NPs, respectively, which enabled the efficient formation of aryl–Cl bonds by working in concert. Interestingly, the unique catalysis of PdAu alloy NPs was positively reflected in the silylation of aryl chlorides, where the reaction of aryl bromides and iodides resulted in low selectivity for the formation of aryl-Si bonds. The results of a kinetic study suggested that specific interaction between PdAu NPs and chloride anion enabled the highly selective silylation of aryl chlorides. Further applications of supported PdAu alloy catalysts in other synthetic reactions involving silylation as well as a theoretical study to reveal the detailed reaction pathway are currently under investigation in our laboratory.

Experimental Section

Materials.

$PdCl_2$ and $HAuCl_4{\cdot}3H_2O$ were purchased from KOJIMA CHEMICALS Co., Ltd. Al_2O_3 (Sumitomo Chemical Co., Ltd, AKP-G015; JRC-ALO-8 equivalent), TiO_2 (JRC-TIO-4), and ZrO_2 (JRC-ZRO-3) were obtained from the Catalysis Society of Japan. $Nb_2O_5{\cdot}nH_2O$ was kindly provided by CBMM. Nb_2O_5 was obtained by the calcination of $Nb_2O_5{\cdot}nH_2O$ at 550 °C for 3 h under air flow. Polyvinyl alcohol (PVA) was purchased from Wako Chemicals. Solvents with super dehydrated grade were used. Aryl chlorides and hydrosilanes were of analytical grade and used as received without further purification.

Physical and Analytical Measurements.

The products of the catalytic runs were analyzed by GC-MS (Shimadzu GCMS-QP2010, CBP-10 capillary column, i.d. 0.25 mm, length 30 m, 50–250 °C) and gas chromatography (Shimadzu GC-2014, CBP-10 capillary column, i.d. 0.25 mm, length 30 m, 50–250 °C). NMR spectra were recorded on a JMN-ECS400 (FT, 400 MHz (^1H), 100 MHz (^{13}C)) instrument (JEOL Ltd., Tokyo, Japan). Chemical shifts (δ) of ^1H and $^{13}C\{^1H\}$ NMR spectra are referenced to $SiMe_4$. The supported catalysts were analyzed by TEM, XRD, XPS and XAFS. High angle annular dark field-scanning transmission electron microscope (HADDF-STEM) images were recorded using a JEOL JEM-3200FS transmission electron microscope. The samples were prepared by depositing drops of ethanol suspensions containing small amounts of the powders onto carbon-coated copper grids (JEOL Ltd.) followed by evaporation of the ethanol in air. X-ray powder diffraction analyses were performed using Cu $K\alpha$ radiation and a one-dimensional X-ray detector (XRD: SmartLab, RIGAKU). The samples were scanned from 2θ=36° to 42° at a scanning rate of 0.067 s^{-1} and a resolution of 0.01°. X-ray photoelectron spectroscopy (XPS) of the catalysts was performed using a JPS-9010 MX instrument. The spectra were measured using MgK_α radiation (15 kV, 400 W) in a chamber at a base pressure of ~10^{-7} Pa. All spectra were calibrated using C_{1s} (284.6 eV) as a reference. Pd K-edge and Au L3-edge XAFS measurements were performed at the BL01B1 beam line at SPring-8 operated at 8 GeV using a Si(311) two-crystal monochromator. XAFS spectra were obtained at room temperature. XANES were analyzed using REX2000 version 2.5 (Rigaku). The actual contents of palladium and gold species immobilized on the supports were determined by atomic emission spectroscopic analysis with a SHIMADZU AA-6200.

Experimental procedure.

Preparation of supported PdAu alloy NPs catalysts by a sol-immobilization method.

Supported PdAu alloy catalysts were prepared through a sol immobilization method. To an aqueous solution (40 mL) containing the desired molar ratio of $PdCl_2$ to $HAuCl_4 \cdot 3H_2O$ was added PVA (36 mg), and the solution was cooled to 273 K with an ice bath. Subsequently, 0.1 M aqueous solution of $NaBH_4$ (8.0 mL, $NaBH_4$/metal (mol/mol) = 5) was added rapidly under vigorous stirring. After 0.5 h of colloid generation, 0.99 g of inorganic support was added to the colloidal solution, which was acidified to pH 1–3 with 0.1 M hydrochloric acid. After vigorous stirring overnight at room temperature, the resulting gray powder was separated from the suspension by centrifugation, thoroughly washed with distilled water, and dried overnight at 80 °C. The obtained catalysts were denoted xPdyAu/support, where x and y indicate the molar ratio of Pd to Au. The total loading amount of metal was set at 5wt%. Supported monometallic Pd and Au catalysts were prepared by the usual impregnation and deposition-precipitation methods, respectively. Supported PdPt alloy catalysts were prepared by a method similar to that used for supported PdAu catalysts with the use of $PdCl_2$ and H_2PtCl_6 as a metal precursor.

General procedure for cross-coupling of aryl chlorides and hydrosilanes over supported PdAu catalyst.

A typical reaction procedure is as follows: **1** (0.50 mmol), **2** (2.5 mmol), Na_2CO_3 (1.0 mmol) and DMA (1.0 mL) were added to a Schlenk tube containing the supported PdAu catalyst (2 mol% as metal) under an Ar atmosphere. The amount of PdAu catalyst used in the catalytic reaction was calculated based on the total amount of the two metals. The progress of the reaction was monitored by GC analysis. After the aryl chloride was completely consumed, the products were quantified by GC using *n*-decane as an internal standard. For isolation of the products, the solid catalyst was removed by passing the mixture through a 0.45 μm polytetrafluoroethylene (PTFE) filter (Millipore Millex LH) The remaining solution was concentrated under reduced pressure and purified through silica gel column chromatography (a mixture of hexane and ethyl acetate) to give the product.

Acknowledgements

This study was supported in part by the Program for Element Strategy Initiative for Catalysts & Batteries (ESICB) (Grant JPMXP0112101003), Platform for Technology and Industry and a Grant-in-Aid for Scientific Research (B) (Grant 17H03459), Early-Career Scientists (Grant 19K15362) and Scientific Research on Innovative Areas (Grant 17H06443) commissioned by MEXT of Japan. The XAFS experiment at SPring–8 was carried out under the approval (proposal Nos. 2018A0910, 2018B1183) of the Japan Synchrotron Radiation Research Institute (JASRI). We wish to thank Mr. Ono of Tokyo Metropolitan University for providing valuable technical support during the HAADF-TEM observations.

References

[1] X.-M. Liu, C. He, J. Huang, J. Xu, *Chem. Mater.* **2005**, *17*, 434–441.
[2] Y. You, C.-G. An, J.-J. Kim, S. Y. Park, *J. Org. Chem.* **2007**, *72*, 6241–6246.
[3] D. Sun, Z. Ren, M. R. Bryce, S. Yan, *J. Mater. Chem. C* **2015**, *3*, 9496–9508.
[4] E. J. Rayment, A. Mekareeya, N. Summerhill, E. A. Anderson, *J. Am. Chem. Soc.* **2017**, *139*, 6138–6145.
[5] S. Bähr, M. Oestreich, *Angew. Chem. Int. Ed.* **2017**, *56*, 52–59; *Angew. Chem.* **2017**, *129*, 52–59.
[6] Z. Xu, W.-S. Huang, J. Zhang, L.-W. Xu, *Synthesis* **2015**, *47*, 3645–3668.
[7] C. Cheng, J. F. Hartwig, *Chem. Rev.* **2015**, *115*, 8946–8975.
[8] R. Sharma, R. Kumar, I. Kumar, B. Singh, U. Sharma, *Synthesis* **2015**, *47*, 2347–2366.
[9] Z. Xu, L.-W. Xu, *ChemSusChem* **2015**, *8*, 2176–2179.
[10] A. A. Toutov, W.-B. Liu, K. N. Betz, A. Fedorov, B. M. Stoltz, R. H. Grubbs, *Nature* **2015**, *518*, 80–84.
[11] Q.-A. Chen, H. F. T. Klare, M. Oestreich, *J. Am. Chem. Soc.* **2016**, *138*, 7868–7871.
[12] Y. Han, S. Zhang, J. He, Y. Zhang, *J. Am. Chem. Soc.* **2017**, *139*, 7399–7407.
[13] Y. Han, S. Zhang, J. He, Y. Zhang, *ACS Catal.* **2018**, *8*, 8765–8773.
[14] M. Murata, K. Suzuki, S. Watanabe, Y. Masuda, *J. Org. Chem.* **1997**, *62*, 8569–8571.
[15] E. Shirakawa, T. Kurahashi, H. Yoshida, T. Hiyama, *Chem. Commun.* **2000**, 1895–1896.
[16] A. S. Manoso, P. DeShong, *J. Org. Chem.* **2001**, *66*, 7449–7455.
[17] S. E. Denmark, J. M. Kallemeyn, *Org. Lett.* **2003**, *5*, 3483–3486.
[18] Y. Yamanoi, *J. Org. Chem.* **2005**, *70*, 9607–9609.
[19] Y. Yamanoi, T. Taira, J. Sato, I. Nakamula, H. Nishihara, *Org. Lett.* **2007**, *9*, 4543–4546.
[20] Y. Kurihara, M. Nishikawa, Y. Yamanoi, H. Nishihara, *Chem. Commun.* **2012**, *48*, 11564–11566.
[21] L. Chen, J.-B. Huang,a Z. Xu, Z.-J. Zheng, K.-F. Yang, Y.-M. Cui, J. Cao, L.-W. Xu, *RSC Adv.* **2016**, *6*, 67113–67117.
[22] Z. Xu, J.-Z. Xu, J. Zhang, Z.-J. Zheng, J. Cao, Y.-M. Cui, L.-W. Xu, *Chem. - Asian J.* **2017**, *12*, 1749–1757.
[23] M. Murata, M. Ishikura, M. Nagata, S. Watanabe, Y. Masuda, *Org. Lett.* **2002**, *4*, 1843–1845.
[24] D. Karshtedt, A. T. Bell, T. D. Tilley, *Organometallics* **2006**, 4471–4482.
[25] Y. Yamanoi, H. Nishihara, *Tetrahedron Lett.* **2006**, *47*, 7157–7161.
[26] M. Murata, H. Yamasaki, T. Ueta, M. Nagata, M. Ishikura, S. Watanabe, Y. Masuda, *Tetrahedron* **2007**, *63*, 4087–4094.
[27] Y. Yamanoi, H. Nishihara, *J. Org. Chem.* **2008**, *73*, 6671–6678.
[28] Z. Tang, Y. Zhang, T. Wang, W. Wang, *Synlett* **2010**, *2010*, 804–808.
[29] A. Hamze, O. Provot, M. Alami, J.-D. Brion, *Org. Lett.* **2006**, *8*, 931–934.
[30] J. Jang, S. Byun, B. M. Kim, S. Lee, *Chem. Commun.* **2018**, *54*, 3492–3495.

[31] A. F. Littke, G. C. Fu, *Angew Chem Int Ed* **2002**, 4176–4211; *Angew. Chem.* **2002**, *114*, 4350–4385.

[32] R. B. Bedford, C. S. J. Cazin, D. Holder, *Coord. Chem. Rev.* **2004**, *248*, 2283–2321.

[33] E. McNeill, T. E. Barder, S. L. Buchwald, *Org. Lett.* **2007**, *9*, 3785–3788.

[34] T. Iwasawa, T. Komano, A. Tajima, M. Tokunaga, Y. Obora, T. Fujihara, Y. Tsuji, *Organometallics* **2006**, *25*, 4665–4669.

[35] A. E. Allen, D. W. C. MacMillan, *Chem. Sci.* **2012**, *3*, 633.

[36] C. S. Schindler, E. N. Jacobsen, *Science* **2013**, *340*, 1052–1053.

[37] W. Guan, G. Zeng, H. Kameo, Y. Nakao, S. Sakaki, *Chem. Rec.* **2016**, *16*, 2405–2425.

[38] D.-S. Kim, W.-J. Park, C.-H. Jun, *Chem. Rev.* **2017**, *117*, 8977–9015.

[39] M. M. Lorion, K. Maindan, A. R. Kapdi, L. Ackermann, *Chem. Soc. Rev.* **2017**, *46*, 7399–7420.

[40] C. Zarate, R. Martin, *J. Am. Chem. Soc.* **2014**, *136*, 2236–2239.

[41] L. Guo, A. Chatupheeraphat, M. Rueping, *Angew. Chem. Int. Ed.* **2016**, *55*, 11810–11813; *Angew. Chem.* **2016**, *128*, 11989–11992.

[42] H. Miura, K. Endo, R. Ogawa, T. Shishido, *ACS Catal.* **2017**, *7*, 1543–1553.

[43] H. Miura, S. Sasaki, R. Ogawa, T. Shishido, *Eur. J. Org. Chem.* **2018**, *2018*, 1858–1862.

[44] H. Miura, Y. Tanaka, K. Nakahara, Y. Hachiya, K. Endo, T. Shishido, *Angew. Chem. Int. Ed.* **2018**, *57*, 6136–6140; *Angew. Chem.* **2018**, *130*, 6244–6248.

[45] K. Nakajima, M. Tominaga, M. Waseda, H. Miura, T. Shishido, *ACS Sustain. Chem. Eng.* **2019**, *7*, 6522–6530.

[46] R. N. Dhital, C. Kamonsatikul, E. Somsook, K. Bobuatong, M. Ehara, S. Karanjit, H. Sakurai, *J. Am. Chem. Soc.* **2012**, *134*, 20250–20253.

[47] B. Boekfa, E. Pahl, N. Gaston, H. Sakurai, J. Limtrakul, M. Ehara, *J. Phys. Chem. C* **2014**, *118*, 22188–22196.

[48] S. Karanjit, A. Jinasan, E. Samsook, R. N. Dhital, K. Motomiya, Y. Sato, K. Tohji, H. Sakurai, *Chem. Commun.* **2015**, *51*, 12724–12727.

[49] R. N. Dhital, K. Bobuatong, M. Ehara, H. Sakurai, *Chem. - Asian J.* **2015**, *10*, 2669–2676.

[50] Structural characterization data of supported PdAu alloy catalysts are summarized in the Supplementary Information.

[51] A. Corma, C. González-Arellano, M. Iglesias, F. Sánchez, *Angew. Chem. Int. Ed.* **2007**, *46*, 7820–7822; *Angew. Chem.* **2007**, 119, 7966–7968.

[52] A. Psyllaki, I. N. Lykakis, M. Stratakis, *Tetrahedron* **2012**, *68*, 8724–8731.

[53] Y. Ishikawa, Y. Yamamoto, N. Asao, *Catal. Sci. Technol.* **2013**, *3*, 2902.

[54] B. S. Takale, S. Wang, X. Zhang, X. Feng, X. Yu, T. Jin, M. Bao, Y. Yamamoto, *Chem Commun* **2014**, *50*, 14401–14404.

[55] M. Kidonakis, M. Stratakis, *Org. Lett.* **2015**, *17*, 4538–4541.

[56] Data for optimization of the reaction conditions are summarized in the Supplementary Information.

FULL PAPER

Silylation of Aryl Chlorides by Bimetallic Catalysis of Palladium and Gold on Alloy Nanoparticles

Adv. Synth. Catal. **Year**, *Volume*, Page – Page

H. Miura,* Y. Masaki, Y. Fukuta, T. Shishido*